Temperature dependence of the Dzyaloshinskii-Moriya interaction in ultrathin films

Yifan Zhou,[1] Rhodri Mansell,[1,*] Sergio Valencia,[2] Florian Kronast,[2] and Sebastiaan van Dijken[1]
[1]*NanoSpin, Department of Applied Physics, Aalto University School of Science, P.O. Box 15100, FI-00076 Aalto, Finland*
[2]*Helmholtz-Zentrum Berlin für Materialien und Energie, Albert-Einstein Str. 15, 12489, Berlin, Germany*

(Received 5 December 2019; revised manuscript received 30 January 2020; accepted 31 January 2020; published 24 February 2020)

The Dzyaloshinskii-Moriya interaction gives rise to a chiral exchange between neighboring spins in the technologically relevant class of perpendicularly magnetized ultrathin film materials. In this paper, we study the temperature dependence of the Dzyaloshinskii-Moriya interaction based on extensive characterization of a thin film which hosts a skyrmion state using both bulk magnetometry and x-ray magnetic circular dichroism photoemission electron microscopy. A version of the Bloch law explicitly for thin film geometries is derived to extract the exchange stiffness. The strength of the Dzyaloshinskii-Moriya interaction, D, is found to have a dependence on the saturation magnetization, M_s of $D \propto M_s^{1.86\pm0.16}$. Further, by extracting the uniaxial anisotropy K_u and the exchange stiffness A, we find that $D \propto K_u^{1.02\pm0.11}$ and $D \propto A^{0.95\pm0.07}$. Skyrmion radii are also used to extract the strength of the Dzyaloshinskii-Moriya interaction which is compared to that derived from measurements of stripe domains. The origins of the correlations between material parameters are discussed and consequences of these relationships for skyrmion devices are considered.

DOI: 10.1103/PhysRevB.101.054433

I. INTRODUCTION

Ultrathin magnetic films enclosed in heterostructures having interfaces with heavy metals or oxides have recently been shown to host technologically interesting magnetic domain walls [1,2] and magnetic skyrmions [3–5]. In particular, the interfacial Dzyaloshinskii-Moriya interaction (DMI) plays a major role in the formation and modulation of magnetic structures [6,7], and is key to various suggested magnetic logic devices [1,8].

The microscopic origins of the DMI are still being investigated. Recent works addressing the relationship between DMI and other material parameters have shown correlations between the DMI and A, the exchange stiffness [9], K_u, the uniaxial magnetic anisotropy [10,11], as well as a strong dependence on M_s, the saturation magnetization [12]. The temperature dependence of these parameters provides a convenient way to investigate their relationships and has been used to gain insight into their physical origin [13–15].

In this paper, we combine bulk magnetometry measurements with high-resolution x-ray magnetic circular dichroism photoemission electron microscopy (XMCD-PEEM) [16] imaging of stripe domains and skyrmions at different temperatures to extract the temperature dependence of the DMI and correlations with M_s, K_u, and A. To extract the exchange stiffness from the measurement of M_s, we derive a version of the Bloch law for the thin film geometry and fit it to our data. We use this data to derive correlations between the parameters and discuss their temperature dependence in relation to the expected temperature-dependent skyrmion stability.

II. EXPERIMENTS AND RESULTS

We study a double magnetic layer structure grown on a Si/SiO_2 substrate with the layer structure Ta (2)/Pt (4)/CoFeB (0.8)/Ru (0.2)/Pt (1)/CoFeB (0.8)/Ru (0.2)/Pt (2) (in nm). The sample has an uniaxial out-of-plane anisotropy, as deduced from Fig. 1(a). The main sources of the perpendicular anisotropy and DMI are the Pt/CoFeB interfaces, with the CoFeB/Ru interfaces mainly acting to break the symmetry of the structure [17].

To obtain the temperature-dependent value of the DMI, we start by extracting M_s and K_u, shown in Fig. 1(b), from hard axis in-plane magnetic hysteresis loops, measured between 150 K and 300 K, after the removal of a linear background contribution due to the sample holder and Si substrate. The value of uniaxial anisotropy K_u is extracted using [15]

$$K_{\text{eff}} = K_u - \mu_0 M_s^2/2, \tag{1}$$

where $\mu_0 {M_s}^2/2$ is the demagnetization energy density corresponding to the thin film geometry and K_{eff} is the effective perpendicular anisotropy as obtained from the in-plane loops. For a bulk-dominated single-site anisotropy, the Callen-Callen relation [18] gives $K_u \propto M_s^3$. However, in thin films such as the one measured here, a two-site anisotropy [15,19] is expected, where the anisotropy is mediated by the adjacent Pt layer, giving $K_u \propto M_s^{\sim 2}$. To obtain the relationship between the two parameters for this film, a linear curve is then fitted to the logarithm of K_u and M_s normalized to their values at 150 K [Fig. 1(c)], which gives a slope of 1.84 ± 0.12, similar to previously reported values from Ta/CoFeB/MgO structures [15,20].

The exchange constant A is another critical parameter in fitting DMI. To extract A, magnetic-field-cooling data, shown in Fig. 1(d), is used. M_s is measured with an in-plane applied

*rhodri.mansell@aalto.fi

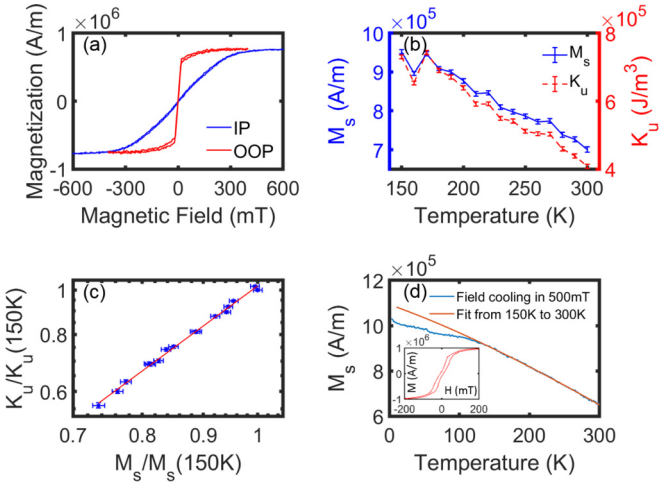

FIG. 1. (a) Hysteresis curve for in-plane (IP) and out-of-plane (OOP) magnetic field direction at 300 K, indicating a perpendicular magnetic anisotropy. (b) Saturation magnetization M_s (left axis) and perpendicular anisotropy K_u (right axis) as a function of temperature from 150 K to 300 K. (c) Log-log plot of K_u versus M_s normalized to their respective values at 150 K. The red line is a linear fit to the data. (d) Fit using the modified Bloch law [Eq. (6)] to field-cooling data taken at 500 mT in-plane applied field. The inset figure shows a multistep out-of-plane hysteresis curve at 100 K.

field of 500 mT and we fit the temperature range 150 K to 300 K. At temperatures below 150 K, we no longer saturate the sample at 500 mT, and we find a two-step out-of-plane hysteresis loop, as shown at 100 K in the inset to Fig. 1(d). This may be caused by interlayer coupling of two CoFeB layers through the thin Pt/Ru spacer [21], and we neglect this region from the fit. At high temperatures, the rate of change of magnetization increases sharply as expected when nearing the Curie temperature T_c, where T_c can be roughly estimated to be 450 K from Fig. 1(d). A low T_c is consistent with the small room temperature M_s of $\sim 6 \times 10^5$ A/m at 300 K, which is around half the bulk value [22].

To extract A from the temperature dependence of the magnetization, the Bloch law [23], derived by calculating the reduction of the magnetization due to excited magnon modes for bulk magnets, is used. Since the Bloch law was derived for bulk magnets, thins films are often fitted using an extra fitting factor or by varying the expected $T^{3/2}$ exponent. However, as noted by Klein and Smith [24], the restriction of spin wave modes in the growth direction should predictably modify the expected temperature dependence. We therefore derive an equation describing the temperature dependence of the magnetization for thin films inspired by the derivation given by Kittel [23] for bulk samples.

At finite temperature, the magnetization of a ferromagnetic thin film is reduced by thermally activated magnons,

$$M_s(T) = M_s(0) - \frac{g\mu_B}{V} \sum_{\boldsymbol{k}} \langle n_{\boldsymbol{k}} \rangle, \tag{2}$$

where g is the gyromagnetic ratio, μ_B is the Bohr magneton, V is volume of the magnetic film, and $\langle n_{\boldsymbol{k}} \rangle$ is the average number of magnons of wave vector $\boldsymbol{k}$. $\langle n_{\boldsymbol{k}} \rangle$ follows Bose-Einstein statistics:

$$\langle n_{\boldsymbol{k}} \rangle = \frac{1}{\exp(E_{\boldsymbol{k}}/k_B T) - 1}. \tag{3}$$

$E_{\boldsymbol{k}}$ is the energy of a magnon and k_B is the Boltzmann constant. Then, at finite temperature, $E_{\boldsymbol{k}}$ can be represented by a thermally excited spin wave, using the nearest-neighbor exchange constant J, magnon spin S, and nearest-neighbor distance a:

$$E_{\boldsymbol{k}} = 4JS(1 - \cos \boldsymbol{k} \cdot a). \tag{4}$$

Assuming a simple cubic structure, this equation can be further simplified in the x and y directions, where the sample dimensions L_x and L_y are much larger than the magnon wavelength, leading to an assumption of continuous $\boldsymbol{k_x}$ and $\boldsymbol{k_y}$, so, for low-energy excitations:

$$E_{\boldsymbol{k_x},\boldsymbol{k_y}} = 2JSk^2 \cdot a^2. \tag{5}$$

In the z direction, as L_z is small, the above assumption is not valid, so that $E_{\boldsymbol{k_z}}$ remains as Eq. (4). By substituting Eqs. (3)–(5) into Eq. (2), converting $\sum_{\boldsymbol{k_x},\boldsymbol{k_x}}$ to $\frac{L_x L_y}{(2\pi)^2} \int_{2\pi/L_{xy}}^{\infty} 2\pi k dk$, and using $S = 1$ as the magnon spin [25], a quantitative relation between $M_s(T)$ and J is obtained:

$$M_s(T) = M_s(0) - \frac{g\mu_B}{L_z} \frac{1}{8\pi Ja^2} k_B T \times \ln\left[1 - \left(1 - \frac{2Ja^2}{k_B T}\left(\frac{2\pi}{L_z}\right)^2\right) \times \sum_{n_z=0}^{L_z/a-1} \exp\left(4J\left(1 - \cos\left(\frac{2\pi}{L_z} n_z\, a\right)\right)\right)\right], \tag{6}$$

where L_{xy} is average length in the x and y directions, L_z is the thickness of the film, and n_z is the number of magnon modes ranging from 0 to $L_z/a - 1$. A similar result is derived by Klein and Smith [24]. This equation is widely applicable to samples in the thin-film limit, allowing J to be extracted by fitting M_s-T data well below T_c.

For the thin CoFeB layer in this paper, the thickness of the magnetic film is $L_z = 0.8$ nm. The following values are extracted from literature: $g = 2.157$ from ferromagnetic resonance measurements [26] and lattice constant $a_0 = 0.288$ nm [27]. We assume that CoFeB adopts a bcc-like CsCl structure, similar to crystalline CoFe [28]. This slightly alters the derivation above leading to a nearest-neighbor distance which is not the lattice constant a_0 but $a = a_0\sqrt{3}/2$. This value is consistent with the measured value of nearest Co and Fe bond distances in thin-film amorphous CoFeB [28]. This leads to the wave vector $\boldsymbol{k}$ having four distinct directions due to eight-nearest neighbors, instead of $\boldsymbol{k_x}$, $\boldsymbol{k_y}$, and $\boldsymbol{k_z}$ in the simple cubic lattice. To use our model with this lattice, we assume the xy plane aligns with the (111) lattice plane of the CsCl lattice. Therefore, of these four wave vectors, two are parallel to the xy plane, and two propagate in the plane normal to the xy plane with a confined number of modes up to $\sqrt{3}L_z/a - 1 \approx 4$.

Thus, the last summation in Eq. (6),

$$\sum_{n_z=0}^{L_z/a-1} \exp\left(4J\left(1-\cos\left(\frac{2\pi}{L_z}n_z\,a\right)\right)\right),$$

is modified to

$$\sum_{n_1=0}^{4}\sum_{n_2=0}^{4} \exp\left(4J\left(1-\cos\left(\frac{2\pi}{\sqrt{3}L_z}(n_1+n_2)\,a\right)\right)\right).$$

Considering all these factors, fitting of the data [Fig. 1(d)] gives a result for zero-temperature exchange constant $J = 3.45 \times 10^{-21}$ J. The fitted exchange constant J can be converted to an exchange stiffness A using [29]

$$A(0) = \frac{1}{2g\mu_B} M_0(2JSa^2). \tag{7}$$

Finally, the temperature dependence of A is considered. Rather than using $A \propto M^2$ as derived from mean-field theory, a correction due to nonlinear spin-wave effects [14] shows that $A(T)$ in a bcc-like structure scales as

$$\frac{A(T)}{A(0)} = \left(\frac{M_s(T)}{M_s(0)}\right)^{1.715}. \tag{8}$$

As a result, A is calculated to be $(6.5 \pm 0.5) \times 10^{-12}$J/m at 300 K. This value is considerably smaller than a more typical value of 2×10^{-11} J/m found in, for instance, a Ta/CoFeB/MgO structure [30]. The difference is likely to be caused by the intermixing of Ru and CoFeB, which has been shown to reduce both A and M_s in Co/Ru multilayers [31].

Due to the existence of models relating the width of magnetic stripe domains in perpendicular samples to the strength of the DMI, we collected a series of stripe domain images at various temperatures using high-resolution XMCD-PEEM, one of which is shown in Fig. 2(a). Images were gathered at the UE49-PGM station at the BESSY synchrotron using contrast from alternating left and right circularly polarized x rays at the Fe-L_3 edge. The average domain width W_d at different temperatures is evaluated by fast-Fourier transforming the images. The radial average of the data in k space is then fitted to a Gaussian distribution, where the peak gives the average length in k. This value is transformed back to real space and the values are plotted in Fig. 2(b).

The stripe domain data, together with K_u, M_s, and A, can be used to extract the DMI by applying the static multilayer domain energy model of Lemesh *et al.* [32] [Eq. (31)]. We assume an initial value of the magnitude of the DMI, D, and calculate the expected domain width W. We then compare W with the experimental value W_d, and vary D until the difference between W and W_d is less than 1 nm. The same sample also gives rise to a skyrmion phase in 2 mT applied out-of-plane field at 280 K, as shown in Fig. 2(c). A few isolated skyrmions are also seen in similar applied fields down to 265 K. By averaging the radial profile extracted from the image for those skyrmions marked by an arrow, the average radius of the skyrmions can be fitted as show in Fig. 2(d), giving $R_{sk} = 102 \pm 5$ nm. To extract a value of D from the skyrmion radius at 280 K we use the model from Wang *et al.* [33] [Eqs. (11) and (12)]. The fitted values of DMI from the stripe domain model are shown as blue points in Fig. 3(a),

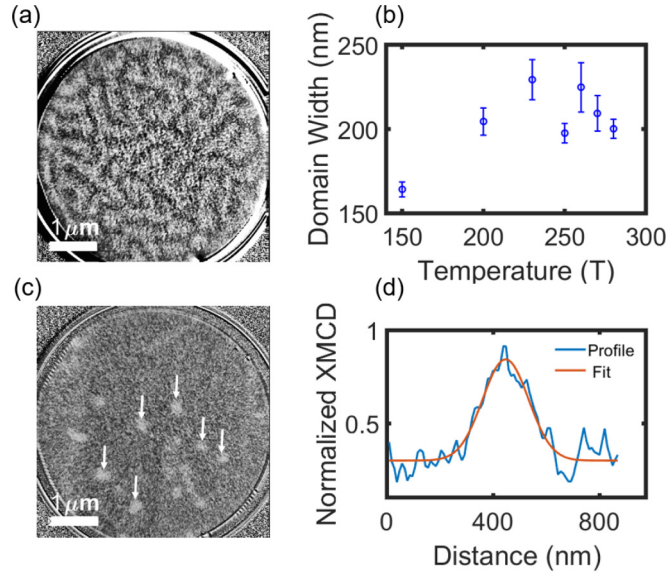

FIG. 2. (a) XMCD image taken at 250 K and 0 mT. (b) The temperature dependence of domain width. (c) Original figure from XMCD of skyrmions in 2 mT at 280 K. The white arrows point at the chosen skyrmions for extracting the skyrmion radius. (d) The Gaussian fitting of the average skyrmion profile from the six chosen skyrmions from (c).

with that extracted from the skyrmion radius shown by the red circle. The value of $D = 1.88 \pm 0.04$ mJ/m^2, for the skyrmion is notably higher than the value obtained from the stripe domain model at the same temperature.

To elucidate the relationship between the DMI and the other variables, double logarithm plots of D with M_s [Fig. 3(b)], A [Fig. 3(c)], and K_u [Fig. 3(d)], are presented. From fits to the data we obtain the relationships $D \propto M_s^{1.86\pm0.16}$, $D \propto K_u^{1.02\pm0.11}$, and $D \propto A^{0.95\pm0.07}$.

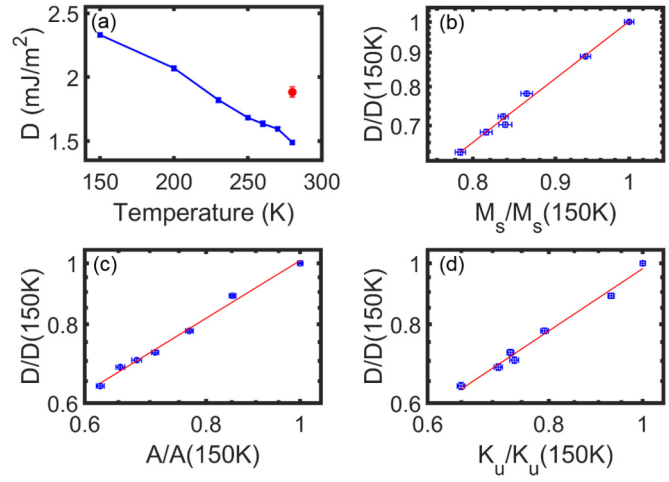

FIG. 3. (a) DMI value from stripe domain model for 150 K to 280 K. The DMI value from the skyrmion model, $D = 1.88 \pm 0.04$ mJ/m^2 at 280 K, is marked as red circle. (b) Log-log plot of DMI with M_s. (c) Log-log plot of DMI with A. (d) Log-log plot of DMI with K_u. The lines in (b)–(d) are linear fits to the data.

III. DISCUSSION AND CONCLUSION

We find, as would be expected, that the DMI decreases with temperature due to thermal disorder. The value of the DMI reported here is similar to previous reports on Co systems with Pt interfaces [12,34,35]. Since even highly ordered Co/Ru interfaces only have weak DMI [36], the observed DMI is likely due to the Pt/CoFeB interface. Previously, in Cu/Co/Pt multilayers measured between 300 K and 600 K, DMI has been found to be proportional to $M_s^{4.9}$, where the higher order relationship was suggested to be the result of changing lattice strain affecting the interfaces at higher temperature [12]. Furthermore, recent theoretical and experimental results have shown a clear dependence of D with A and K_u. Looking first at A, the linear dependence of DMI and exchange has been shown in an in-plane Permalloy system [9] and perpendicular Pt/Co/MgO multilayers [10], consistent with the results presented here. This linear dependence indicates that the asymmetric and symmetric exchange interactions have a similar temperature scaling, in agreement with theoretical calculations based on the spin wave spectrum at finite temperatures [37].

A linear dependence of D on K_u has also been reported in a perpendicular AlO_x/Co/Pt structure [11]. Recent works have demonstrated that the hybridization of electron orbitals at the interface causing asymmetry in the orbital magnetic moment correlates with interfacial DMI [38–40]. In our multilayer system, we find that D and K_u are linearly dependent as well. Whilst a double-layer structure was studied here, we expect that the results will generalize to single layers and multilayers, particularly due to the dominance of the interfaces and the similarity of the temperature dependencies found across different systems.

The temperature-dependence of DMI in thin films is important for possible applications for spintronic devices. All possible devices will be expected to work across a well-defined temperature range. For skyrmion-based devices, we can use the calculation by Wang *et al.* [33] for zero-field skyrmions to investigate the temperature dependence. Wang *et al.* derive an expression for the zero-field skyrmion radius as

$$R_{\mathrm{sk}} = \pi D \sqrt{\frac{A}{16AK_{\mathrm{eff}}^2 - \pi^2 D^2 K_{\mathrm{eff}}}}, \tag{9}$$

which gives a condition for the stability of a zero-field skyrmion as

$$16AK_{\mathrm{eff}} > \pi^2 D^2. \tag{10}$$

Using our results for the temperature dependence, we find that the stability criterion is not strongly temperature dependent. We find that between 150 and 300 K, the effective anisotropy $K_{\mathrm{eff}} \propto M_s^{1.7}$, so the term $AK_{\mathrm{eff}} \propto M_s^{3.4}$ whilst $D^2 \propto M_s^{3.7}$, meaning that the required relationship between A, K_{eff}, and D only gradually changes with temperature. Similarly for the skyrmion radius, only a limited temperature dependence is expected. Some experimental confirmation of this may be found in Raju *et al.* [41], where similar-sized skyrmions are imaged between 5 K and 200 K. Therefore, although in the range studied here we find a roughly 50% change in DMI over a range of 130 K, this does not necessarily translate into a large change in the size and stability of skyrmions.

A further complication for devices is the large apparent spatial variation of DMI. Both here and in a previous work comparing the average DMI derived from stripe domains to that at skyrmion sites [34], a distinct difference between the bulk- and skyrmion-obtained DMI has been found. However, given the small area of the sample covered by skyrmions and assuming that the skyrmions will tend to be pinned at the sites of highest DMI [34], the difference is still consistent with a Gaussian distribution of DMI with a standard deviation of around 15–20% of the mean. Further work is required to understand and control the distribution of the DMI, as well as spatial correlations with changes in the other material parameters.

In conclusion, we find that the temperature scaling of interfacial DMI follows $D \propto M_s^{1.86\pm0.16}$, with near-linear correlations to both the exchange stiffness A and uniaxial anisotropy, K, in agreement with previous works. To extract the exchange stiffness, a version of the Bloch law relevant to the thin film geometry was derived. The results show that manipulation of exchange stiffness, as is done here through the Ru layer, may also be an effective way of manipulating the thin film magnetic properties. The relationships between the variables mean that a fairly weak temperature dependence of the existence and size of skyrmions in such films is expected, which is promising for device applications.

ACKNOWLEDGMENTS

We acknowledge funding from the Academy of Finland (Grant Nos. 295269, 306978, 319217 and 327804) as well as support from Helmholtz-Zentrum Berlin (HZB) for synchrotron beamtime at the UE49-PGM SPEEM beamline (Proposal No. 18106805) and the project CALIPSOplus under Grant Agreement No. 730872 from the EU Framework Programme for Research and Innovation HORIZON 2020.

[1] K.-S. Ryu, L. Thomas, S.-H. Yang, and S. S. Parkin, Nat. Nanotechnol. **8**, 527 (2013).

[2] M. Benitez, A. Hrabec, A. Mihai, T. Moore, G. Burnell, D. McGrouther, C. Marrows, and S. McVitie, Nat. Commun. **6**, 8957 (2015).

[3] J. Zang, M. Mostovoy, J. H. Han, and N. Nagaosa, Phys. Rev. Lett. **107**, 136804 (2011).

[4] W. Jiang, P. Upadhyaya, W. Zhang, G. Yu, M. B. Jungfleisch, F. Y. Fradin, J. E. Pearson, Y. Tserkovnyak, K. L. Wang, O. Heinonen, S. G. te Velthuis, and A. Hoffmann, Science **349**, 283 (2015).

[5] W. Jiang, X. Zhang, G. Yu, W. Zhang, X. Wang, M. B. Jungfleisch, J. E. Pearson, X. Cheng, O. Heinonen, K. L. Wang, Y. Zhou, A. Hoffmann, and S. G. E. te Velthuis, Nat. Phys. **13**, 162 (2017).

[6] S. Rohart and A. Thiaville, Phys. Rev. B **88**, 184422 (2013).

[7] M. Heide, G. Bihlmayer, and S. Blügel, Phys. Rev. B **78**, 140403(R) (2008).

[8] A. Fert, V. Cros, and J. Sampaio, Nat. Nanotechnol. **8**, 152 (2013).

[9] H. T. Nembach, J. M. Shaw, M. Weiler, E. Jué, and T. J. Silva, Nat. Phys. **11**, 825 (2015).

[10] S. Kim, K. Ueda, G. Go, P.-H. Jang, K.-J. Lee, A. Belabbes, A. Manchon, M. Suzuki, Y. Kotani, T. Nakamura, K. Nakamura, T. Koyama, D. Chiba, K. T. Yamada, D.-H. Kim, T. Moriyama, K. Kab-Jin, and T. Ono, Nat. Commun. **9**, 1648 (2018).

[11] N.-H. Kim, D.-S. Han, J. Jung, K. Park, H. J. Swagten, J.-S. Kim, and C.-Y. You, Appl. Phys. Express **10**, 103003 (2017).

[12] S. Schlotter, P. Agrawal, and G. S. Beach, Appl. Phys. Lett. **113**, 092402 (2018).

[13] R. Moreno, R. F. L. Evans, S. Khmelevskyi, M. C. Muñoz, R. W. Chantrell, and O. Chubykalo-Fesenko, Phys. Rev. B **94**, 104433 (2016).

[14] U. Atxitia, D. Hinzke, O. Chubykalo-Fesenko, U. Nowak, H. Kachkachi, O. N. Mryasov, R. F. Evans, and R. W. Chantrell, Phys. Rev. B **82**, 134440 (2010).

[15] H. Sato, P. Chureemart, F. Matsukura, R. W. Chantrell, H. Ohno, and R. F. L. Evans, Phys. Rev. B **98**, 214428 (2018).

[16] F. Kronast and S. Valencia Molina, Journal of Large-Scale Research Facilities JLSRF **2**, 90 (2016).

[17] M. Belmeguenai, H. Bouloussa, Y. Roussigné, M. S. Gabor, T. Petrisor Jr., C. Tiusan, H. Yang, A. Stashkevich, and S. M. Chérif, Phys. Rev. B **96**, 144402 (2017).

[18] H. B. Callen and E. Callen, J. Phys. Chem. Solids **27**, 1271 (1966).

[19] O. N. Mryasov, U. Nowak, K. Y. Guslienko, and R. W. Chantrell, Europhys. Lett. **69**, 805 (2005).

[20] J. G. Alzate, P. Khalili Amiri, G. Yu, P. Upadhyaya, J. A. Katine, J. Langer, B. Ocker, I. N. Krivorotov, and K. L. Wang, Appl. Phys. Lett. **104**, 112410 (2014).

[21] R. Lavrijsen, A. Fernández-Pacheco, D. Petit, R. Mansell, J. Lee, and R. Cowburn, Appl. Phys. Lett. **100**, 052411 (2012).

[22] K.-M. Lee, J. W. Choi, J. Sok, and B.-C. Min, AIP Adv. **7**, 065107 (2017).

[23] C. Kittel, *Introduction to Solid State Physics* (Wiley, New York, 1966).

[24] M. J. Klein and R. S. Smith, Phys. Rev. **81**, 378 (1951).

[25] S. Blundell, *Magnetism in Condensed Matter* (Oxford University Press, Oxford, UK, 2003).

[26] T. Devolder, P.-H. Ducrot, J.-P. Adam, I. Barisic, N. Vernier, J.-V. Kim, B. Ockert, and D. Ravelosona, Appl. Phys. Lett. **102**, 022407 (2013).

[27] R. Lavrijsen, P. Paluskar, C. Loermans, P. van Kruisbergen, J. Kohlhepp, H. Swagten, B. Koopmans, and E. Snoeck, J. Appl. Phys. **109**, 093905 (2011).

[28] D. Kirk, A. Kohn, K. B. Borisenko, C. Lang, J. Schmalhorst, G. Reiss, and D. J. H. Cockayne, Phys. Rev. B **79**, 014203 (2009).

[29] C. Vaz, J. Bland, and G. Lauhoff, Rep. Prog. Phys. **71**, 056501 (2008).

[30] T. Devolder, J.-V. Kim, L. Nistor, R. Sousa, B. Rodmacq, and B. Diény, J. Appl. Phys. **120**, 183902 (2016).

[31] C. Eyrich, A. Zamani, W. Huttema, M. Arora, D. Harrison, F. Rashidi, D. Broun, B. Heinrich, O. Mryasov, M. Ahlberg, O. Karis, P. E. Jönsson, M. From, X. Zhu, and E. Girt, Phys. Rev. B **90**, 235408 (2014).

[32] I. Lemesh, F. Büttner, and G. S. D. Beach, Phys. Rev. B **95**, 174423 (2017).

[33] X. Wang, H. Yuan, and X. Wang, Commun. Phys. **1**, 31 (2018).

[34] M. Baćani, M. A. Marioni, J. Schwenk, and H. J. Hug, Sci. Rep. **9**, 3114 (2019).

[35] P. Agrawal, F. Büttner, I. Lemesh, S. Schlotter, and G. S. D. Beach, Phys. Rev. B **100**, 104430 (2019).

[36] M. Hervé, B. Dupé, R. Lopes, M. Böttcher, M. D. Martins, T. Balashov, L. Gerhard, J. Sinova, and W. Wulfhekel, Nat. Commun. **9**, 1015 (2018).

[37] L. Rózsa, U. Atxitia, and U. Nowak, Phys. Rev. B **96**, 094436 (2017).

[38] H. Yang, A. Thiaville, S. Rohart, A. Fert, and M. Chshiev, Phys. Rev. Lett. **115**, 267210 (2015).

[39] N. Nakajima, T. Koide, T. Shidara, H. Miyauchi, H. Fukutani, A. Fujimori, K. Iio, T. Katayama, M. Nývlt, and Y. Suzuki, Phys. Rev. Lett. **81**, 5229 (1998).

[40] H. T. Nembach, E. Jué, E. R. Evarts, and J. M. Shaw, Phys. Rev. B **101**, 020409(R) (2020).

[41] M. Raju, A. Yagil, A. Soumyanarayanan, A. K. C. Tan, A. Almoalem, F. Ma, O. M. Auslaender, and C. Panagopoulos, Nat. Commun. **10**, 696 (2019).